



Published in final edited form as:

Magn Reson Med. 2018 May ; 79(5): 2451–2459. doi:10.1002/mrm.27122.

Probing cardiac metabolism by hyperpolarized ^{13}C MR using an exclusively endogenous substrate mixture and photo-induced non-persistent radicals

Jessica A. M. Bastiaansen^{1,2,3}, Hikari A. I. Yoshihara^{2,4}, Andrea Capozzi⁵, Juerg Schwitter⁴, Rolf Gruetter³, Matthew E. Merritt⁶, and Arnaud Comment^{2,7}

¹Department of Radiology, University Hospital Lausanne (CHUV) and University of Lausanne (UNIL), Lausanne, Switzerland ²Institute of Physics, Ecole Polytechnique Fédérale de Lausanne, Lausanne, Switzerland ³Laboratory of Functional and Metabolic Imaging, EPFL, Lausanne, Switzerland ⁴Division of Cardiology and Cardiac MR Center, University Hospital Lausanne (CHUV), Lausanne, Switzerland ⁵Department of Electrical Engineering, Technical University of Denmark, Copenhagen, Denmark ⁶Department of Biochemistry and Molecular Biology, University of Florida, Gainesville, FL 32610, USA ⁷General Electric Healthcare, Pollards Wood, Nightingales Lane, Chalfont St Giles, Buckinghamshire, HP8 4SP, United Kingdom

Abstract

Purpose—To probe the cardiac metabolism of carbohydrates and short chain fatty acids simultaneously *in vivo* following the injection of a hyperpolarized ^{13}C -labeled substrate mixture prepared using photo-induced non-persistent radicals.

Methods—Droplets of mixed [$1-^{13}\text{C}$]pyruvic and [$1-^{13}\text{C}$]butyric acids were frozen into glassy beads in liquid nitrogen. Ethanol addition was investigated as a means to increase the polarization level. The beads were irradiated with ultraviolet (UV) light and the radical concentration was measured by ESR spectroscopy. Following dynamic nuclear polarization (DNP) in a 7T polarizer, the beads were dissolved, and the radical-free hyperpolarized solution was rapidly transferred into an injection pump located inside a 9.4T scanner. The hyperpolarized solution was injected in healthy rats to measure cardiac metabolism *in vivo*.

Results—UV-irradiation created non-persistent radicals in a mixture containing ^{13}C -labeled pyruvic and butyric acids and enabled the hyperpolarization of both substrates by DNP. Ethanol addition increased the radical concentration from 16 to 26 mM. Liquid-state ^{13}C polarization was 3% inside the pump at the time of injection, and increased to 5% by addition of ethanol to the substrate mixture prior to UV irradiation. In the rat heart, the *in vivo* ^{13}C signals from lactate, alanine, bicarbonate and acetylcarnitine were detected following the metabolism of the injected substrate mixture.

*Correspondence: Jessica AM Bastiaansen, Department of Radiology, University Hospital Lausanne (CHUV), Rue de Bugnon 46, BH 8.84, 1011 Lausanne, Switzerland, Phone: +41-21-3147516, jbastiaansen.mri@gmail.com. Arnaud Comment, General Electric Healthcare, Pollards Wood, Nightingales Lane, Chalfont St Giles, Buckinghamshire, HP8 4SP, United Kingdom, arnaud.comment@ge.com.

Competing financial interests

Arnaud Comment is currently employed by General Electric Medical Systems, Inc.

Conclusion—Co-polarization of two ^{13}C -labeled substrates and the detection of their myocardial metabolism *in vivo* was achieved without using persistent radicals. The absence of radicals in the solution containing the hyperpolarized ^{13}C -substrates may simplify the translation to clinical use because no filtration is required prior to injection.

Keywords

metabolic imaging; carbon-13; hyperpolarization; energy metabolism; oxidative metabolism

INTRODUCTION

Hyperpolarization methods overcome the relatively low sensitivity of magnetic resonance spectroscopy (MRS), and by combining dissolution dynamic nuclear polarization (DNP) (1) and ^{13}C MRS imaging, *in vivo* metabolism can be probed in real time (2). Hyperpolarized ^{13}C MR has already been extensively used in a wide range of preclinical models, where it was shown to be sensitive to variations in key metabolic pathways (3–8). The technique has recently been translated to studies investigating prostate cancer and heart disease in human subjects (9,10). Further clinical applications in cardiology and oncology have been discussed (11,12), and several sites around the world are now poised to initiate clinical trials.

Because of the heart's high substrate uptake rate, cardiac applications are well adapted to the relatively short life time of the hyperpolarized ^{13}C MR signals. Heart metabolism is flexible, exhibiting the ability to switch between the oxidation of different substrates, depending on their availability and metabolic state, but substrate preference is often disturbed and shifted in disease (13). Using hyperpolarized ^{13}C MR, it was recently shown that both short chain fatty acid and carbohydrate oxidation can be simultaneously monitored *in vivo*, in real time, and in a single experiment, following the co-administration of two different substrates (14). However, this promising substrate mixture has not yet been validated for clinical applications, and the initial preclinical experiments were done using nitroxyl radicals.

In order to hyperpolarize the ^{13}C spins by means of DNP, it is necessary to admix persistent radicals with the ^{13}C -labeled biomolecules of interest (1). These radicals must be removed prior to injection into humans, and the polarization of pyruvic acid for clinical applications is currently performed with a specific form of costly trityl radical that can be extracted from an acidic solution (15). The inline filtration process might however be more challenging for complex mixtures of biomolecules. For regulatory reasons it is also necessary to add a quality control test to ensure that the filtration process was efficient and that the residual concentration of radical is below an acceptable value, a step that adds complexity to the process, possibly delaying the release of the hyperpolarized ^{13}C substrates for injection, and that can potentially fail.

It was recently demonstrated that it is possible to perform DNP using non-persistent radicals induced by UV irradiation of pyruvic acid (16). These radicals can be used to efficiently hyperpolarize $[1-^{13}\text{C}]$ pyruvic acid as well as other ^{13}C -biomolecules and isotopes with nuclear spin (16,17). The radicals disappear upon dissolution, recombining to form $^{13}\text{CO}_2$ and unlabeled acetate (16). As a result, the hyperpolarized solution can be formulated to contain only endogenous substrates. The use of photo-induced non-persistent radicals may

also reduce experimental costs as they alleviate the need for synthetic persistent radicals. Another promising development recently demonstrated that photo-induced radicals can be annihilated without dissolving the frozen substrates, allowing storage and transport of hyperpolarized substances (18). This may lead to a paradigm shift in DNP, providing applications for sites that are not equipped with their own DNP equipment to perform clinical studies.

The purpose of the present work was to investigate whether photo-induced non-persistent radicals could be used to co-polarize a mixture of ^{13}C -substrates for the simultaneous measurement of separate biochemical pathways *in vivo*.

METHODS

Sample preparation

All chemicals were purchased from Sigma-Aldrich, Buchs, Switzerland. A solution composed of 50 μL [$1\text{-}^{13}\text{C}$]pyruvic acid and 50 μL [$1\text{-}^{13}\text{C}$]butyric acid was pipetted dropwise in liquid nitrogen to form frozen glassy beads of $\sim 10\ \mu\text{L}$ (diameter of $\sim 2.5\ \text{mm}$) which were collected inside the 6-mm-inner-diameter tail of a quartz dewar designed for electron spin resonance (ESR) measurements (Wilma 150-mL Suprasil Dewar Flask type WG-850-B-Q). The frozen beads were then irradiated with ultraviolet (UV) light for a total of 1 h using a 365-nm LED array (Hamamatsu LC-L5) following a previously-described procedure (17). This process creates the radicals necessary for DNP. After completion of the irradiation, the beads were transferred to a glass vial for storage in liquid nitrogen. It was also investigated whether radical concentration and polarization level can be increased by modifying the substrate mixture according to (17). Therefore, a second solution composed of [$1\text{-}^{13}\text{C}$]pyruvic acid, [$1\text{-}^{13}\text{C}$]butyric acid, and ethanol in a 2:2:1 ratio (v/v) was prepared separately. The mixture containing ethanol was however not used for *in vivo* experiments.

Radical concentration measurements

In a separate set of experiments, the radical concentration was measured as a function of the UV irradiation time using an X-band ESR spectrometer (Bruker EMX, Billerica, Massachusetts, USA) (17). Measurements were performed at 77 K on frozen UV-irradiated beads containing only [$1\text{-}^{13}\text{C}$]pyruvic and [$1\text{-}^{13}\text{C}$]butyric acid, as well as in UV-irradiated beads containing an added 20% volume of ethanol. ESR measurements of the UV-irradiated mixtures were performed at 10 min intervals during the 1h irradiation process and the radical concentration was plotted as a function of the total irradiation time.

Polarization and dissolution

The frozen glassy UV-irradiated beads were loaded into a polytetrafluoroethylene (PTFE) sample cup together with frozen droplets of NaOH solution, the volume and concentration of which was calculated to balance the pH to 7 during dissolution. The PTFE cup was then placed inside a 7 T homebuilt polarizer and the ^{13}C spins were polarized for 2 h at $1.0 \pm 0.1\ \text{K}$ with the microwave frequency set to 196.75 GHz (19–21). Using an automated process (22), the sample was rapidly dissolved in 6 mL D_2O and transferred within 2 s into a remotely-controlled phase separator/injection pump (23), located inside the bore of the MR scanner

(Fig. 1). For the *in vivo* experiments, the separator/injection pump was prefilled with 0.6 mL of phosphate buffered saline and heparin, and, 800 μ L of the hyperpolarized ^{13}C -labeled substrate mixture was automatically injected into the femoral vein of the animal.

In vitro hyperpolarized and thermal ^{13}C MRS

In vitro experiments were performed to determine the ^{13}C signal enhancement and polarization levels for both types of UV-irradiated mixtures after hyperpolarization and transfer into the separator/injection pump. All *in vitro* ^{13}C MRS measurements were performed within the pump as previously described (22) using a custom-made dual $^1\text{H}/^{13}\text{C}$ probe wrapped around the body of the pump. The hyperpolarized ^{13}C MRS acquisition was triggered at the start of the infusion process, collecting transient spectra with a 3 s repetition time and radiofrequency (RF) excitation angle of 5° . Two different quantitative methods were used to measure the thermal ^{13}C polarization to doubly verify the polarization levels obtained after dissolution as each method may be subject to different potential sources of error (see Supporting Methods): first, the ^{13}C signal was measured using 90° RF excitation pulses with a repetition time of 240 s and 8 averages as described previously (24). The second method consisted in measuring the ^{13}C signal with a 5° RF excitation angle, repetition time of 1.1 s and 1024 averages following the addition of 5 μ L of gadolinium complex (1 mmol/mL, Dotarem[®], gadoteric acid, 0.5M, Guerbet) to a concentration of \sim 1 mM as described previously (21).

Animals

All animal experiments were conducted according to federal ethical guidelines and were approved by the local regulatory body. Male Sprague Dawley rats were initially anesthetized with 5% isoflurane in oxygen. Catheters were placed into the femoral vein for substrate delivery and in the femoral artery to monitor the blood pressure and heart rate as previously described (25,26). The respiration rate, cardiac rhythm, and temperature were monitored and maintained using respectively a pneumatic respiration sensor, a blood pressure sensor, and a rectal temperature probe (Small Animal Instruments, Inc., Stony Brook, NY, USA). After surgery, the isoflurane concentration was decreased to 1.5% in oxygen. Animals were placed supine in a custom-designed animal holder and heating was provided by warm water circulating through tubing placed next to the rat.

In vivo MRI and hyperpolarized ^{13}C MRS

All MRI and MRS measurements were carried out in a horizontal bore 9.4 T magnet (Magnex Scientific, Oxford, UK) with a Direct Drive spectrometer (Varian, Palo Alto, CA, USA). A custom-made radiofrequency (RF) hybrid probe, consisting of a 10 mm diameter proton surface coil and a pair of 10 mm diameter ^{13}C surface coils in quadrature mode, was positioned over the chest of the rat for transmission and reception. A hollow glass sphere with a 3 mm inner diameter (Wilmad-LabGlass, NJ, USA) was filled with an aqueous 1 M [$1\text{-}^{13}\text{C}$]glucose solution and used to adjust the radiofrequency (RF) excitation pulse power and set the reference frequency. Acquisition of gradient echo proton images confirmed the correct placement of the coil and was used to determine the voxel used for shimming.

Cinematographic images (FOV = 40 x 40 mm²; matrix size: 256 x 256; repetition time (TR) = 140 ms; echo time (TE) = 4.5 ms; NA = 8; number of frames: 14; slice thickness: 1 mm) were acquired to confirm and set the timing of the cardiac trigger in the end-diastolic phase. The cardiac trigger was typically sent 50 or 60 ms after the observed maximum blood pressure. Cardiac-triggered and respiratory-gated shimming was performed using the FAST(EST)MAP gradient shimming routine (27) to reduce the localized proton line width in a myocardial voxel of 4 x 5 x 5 mm³ (acquired by stimulated echo localized spectroscopy) to 20 – 30 Hz, resulting in a non-localized proton line width of 80 – 120 Hz. The MR console was triggered to start acquisition at the beginning of the automated injection process of the hyperpolarized ¹³C substrate mixture. Series of single pulse acquisitions were sequentially recorded using 30° adiabatic RF excitation pulses (BIR-4) (28), with ¹H decoupling using WALTZ (29). Free induction decays were acquired with 4129 complex data points over a 20 kHz bandwidth. All acquisitions were cardiac triggered and respiratory gated, resulting in a TR between 3 and 3.5 s. The adiabatic pulse offset and power were calibrated to ensure that the RF excitation angle $\theta = 30^\circ$ for all observed metabolites in the entire tissue of interest.

Data analysis and statistics

¹³C signal integrals were quantified with Bayes (Washington University, St. Louis, MO, USA) as previously described (30). All metabolite signal integrals were normalized to the respective substrate signal integral. Statistics on the comparison between polarization levels obtained with and without the addition of ethanol to the substrate mixture were computed via two-tailed Student's t-tests for unpaired data with equal variance. All data are expressed as mean ± standard error of the mean (SEM).

RESULTS

To measure *in vivo* cardiac metabolism of different substrates simultaneously, without adding persistent radicals, it was demonstrated that co-polarization of both ¹³C-labeled butyric and pyruvic acids is possible using photo-induced non-persistent radicals. The radicals created at 77 K by UV irradiation of pyruvic acid act as polarizing agents for both acids. The presence of butyric acid did not modify the structure of the UV-induced radical, based on the ESR spectral analysis. Since the radicals are scavenged during the dissolution process, a radical-free hyperpolarized ¹³C labeled substrate mixture was obtained and could be injected for *in vivo* real-time metabolic measurements.

To assess the concentration of radicals, ESR measurements were performed at several time points during the irradiation process, which indicated that the maximum concentration of radicals was obtained after 1 h of irradiation, regardless of the composition of the mixture (Fig. 2a). The solution containing solely ¹³C substrates reached a maximum radical concentration of 16 mM (Fig. 2a). The solution where ethanol was added to a concentration of 20% (v/v) reached a maximum radical concentration of 26 mM (Fig. 2a), a significant increase in radical concentration compared with the mixture of only pyruvic and butyric acid.

To assess the degree of achieved hyperpolarization, *in vitro* hyperpolarized and thermally polarized ^{13}C MRS experiments were performed on both mixtures and a mean ^{13}C enhancement of 4'100 and 6'400 (Fig. 2b) was observed. A ^{13}C mean polarization of $3.3\pm 0.5\%$ and $5.2\pm 0.5\%$ (Fig. 2c) was measured for the undoped mixture and the ethanol-doped mixture, respectively. The addition of ethanol to the substrate mixture led to a significant increase in the measured polarization level (Fig. 2b and 2c, $p=0.03$). As expected, the two different methods used to measure the thermally polarized ^{13}C resonances did not lead to significantly different estimations of the ^{13}C polarization (Supporting Table S1). Both the HP time courses (Fig. 2d) of $[1-^{13}\text{C}]$ pyruvic and $[1-^{13}\text{C}]$ butyric acid as well as the summed spectrum (Fig. 2e) show a higher signal intensity of the C1 label of pyruvic acid compared with that of butyric acid, which corresponds to the different concentrations of the compounds when mixed in equal volumes. The difference in enhancement between the thermally polarized substrates versus the hyperpolarized substrates was evident in both spectra (Fig. 2e).

To assess if *in vivo* metabolism could be observed, the UV-irradiated mixture containing only $[1-^{13}\text{C}]$ pyruvic and $[1-^{13}\text{C}]$ butyric acid was injected in 5 healthy animals. The myocardial metabolism of the hyperpolarized UV-irradiated mixture was followed in real time (Fig. 3a), showing that sufficient polarization levels were obtained to measure metabolic processes using this radical-free method. The metabolism of hyperpolarized $[1-^{13}\text{C}]$ pyruvate led to the detection of lactate, alanine, and ^{13}C bicarbonate (Fig. 3b). Metabolism of hyperpolarized butyrate resulted in ^{13}C labeling in acetylcarnitine (Fig. 3b). The ratio of acetylcarnitine relative to injected substrate butyrate was 0.011 ± 0.004 , the lactate-to-pyruvate ratio was 0.068 ± 0.023 , the alanine-to-pyruvate ratio was 0.029 ± 0.008 , and the bicarbonate-to-pyruvate ratio was 0.006 ± 0.001 (Fig. 4).

DISCUSSION

In the present study we show for the first time the measurement of myocardial metabolism using DNP with photo-induced non-persistent radicals. Metabolic conversion of the injected substrate mixture resulted in the ^{13}C labeling and *in vivo* measurement of acetylcarnitine, bicarbonate and lactate. Although the ^{13}C polarization levels observed in this study were not as large as those obtained with persistent radicals, we demonstrated that multiple ^{13}C -labeled substrates could be co-polarized in UV-irradiated mixtures containing pyruvic and butyric acid and that the mixture could be used for *in vivo* cardiac metabolic studies in rats. The use of non-persistent radicals may reduce cost and also simplify the preparation process of hyperpolarized ^{13}C -substrates mixtures for *in vivo* applications, notably by removing the need for a filter, which could also allow reducing the delay between dissolution and injection. This shows that the noninvasive and simultaneous measurement of metabolic substrate competition can be measured in the heart in a single experiment without addition of exogenous persistent radicals or glassing solvents, thus facilitating the translation of these types of experiments to humans (31).

In vivo metabolic measurements using hyperpolarized ^{13}C MRS following the administration of UV-irradiated mixtures were compared to the ^{13}C spectra acquired after injection of mixtures that were hyperpolarized with persistent radicals (TEMPO) (14) to

illustrate the impact of the difference in ^{13}C polarization (Fig. 5). Although our study with the persistent TEMPO radicals generated a larger ^{13}C polarization ($13\pm 2\%$ at time of injection (14)), similar metabolite ratios were observed in the current study using UV-induced non-persistent radicals, albeit with different SNR levels. Both studies were conducted under identical experimental conditions with *in vivo* femoral vein injections starting 3 seconds after dissolution. One of the consequences of the larger ^{13}C polarization obtained in our study with the persistent radicals was that the ^{13}C labeling of glutamate and acetoacetate could be observed (14), but it must be kept in mind that there was no attempt to filter or scavenge the nitroxyl radicals which were injected together with the substrates. Note also that because of the spectral overlap with metabolites originating from pyruvate metabolism, the resonances of β -hydroxybutyrate and citrate, which have been observed in previous studies using hyperpolarized butyrate and persistent radicals could not be observed (14,32). However, the wide versatility of photo-induced non-persistent radicals permits the hyperpolarization of substrate mixtures containing unlabeled pyruvic acid. Because of substrate competition, changes in utilization may occur with co-infusion of carbohydrates and fatty acids (14) but this may be exploited to study specific metabolic phenotypes.

The total amount of acetate in the hyperpolarized solution is equivalent to the number of photo-induced radicals (16 mM) created in the frozen sample (100 μL) (16). After dissolution and infusion, we estimate this increases the blood acetate concentration by 10 μM . Since rats typically have 200 μM acetate in blood (33), and based on our earlier studies of ^{13}C labeled acetate conversion to ^{13}C acetylcarnitine in muscle (25,26), the minor contribution of unlabeled acetate was considered to have negligible effects on the acetylcarnitine pool size.

The SNR and polarization level obtained in these experiments were sufficient to detect the downstream metabolites acetylcarnitine, bicarbonate and lactate, but a higher SNR would be required for detecting other metabolites and would be beneficial for imaging applications. The liquid-state ^{13}C polarization obtained in the present study was considerably lower ($\sim 3.3\%$) than the maximum achieved previously using TEMPO ($\sim 13\%$) (14). Since nitroxyl radicals show a broader ESR spectrum if compared to the one arising from UV-irradiated pyruvic acid (17), the lower DNP enhancement must result from the non-optimal concentration of paramagnetic centers for the temperature and magnetic field strength. Indeed, as illustrated by the addition of ethanol to the pyruvic and butyric acid mixture, increasing the radical concentration from 16 mM to 26 mM improved the polarization from 3.3% to 5.1%, demonstrating that it is possible to increase the ^{13}C polarization this way. It was already previously reported that diluting pyruvic acid in a polar solvent increased the radical concentration above 20 mM (17). Besides the effect on radical yield, ethanol addition may also enhance polarization by improving the glassing. The increased radical concentration is particularly beneficial to the DNP process when working at high magnetic field as was done in the current study. However, to avoid any additional metabolic perturbation, the ethanol mixtures were not used for the *in vivo* cardiac experiments.

Preliminary results show that the utilization of a broadband UV source also dramatically improves the maximum radical yield (18). At this high field, given the width of the UV-PA radical spectrum compared to TEMPO (17), modulating the microwave frequency might be

beneficial for improving the polarization level and reducing the build-up time (34). However, since all these potential improvements require additional hardware, the development of these methods to increase the ^{13}C polarization was beyond the scope of this study.

There are several advantages to the use of photo-induced non-persistent radicals: besides cost-reduction, the removal of the filtration step would simplify the production process of hyperpolarized substrates for clinical applications and may improve its robustness. In addition, as was recently demonstrated with hyperpolarized $[1-^{13}\text{C}]$ pyruvic acid (18), the use of photo-induced radicals allows for the storage of hyperpolarized substrates and may enable their transport to another location, which is of particular interest for clinical studies at sites without DNP equipment. Our results demonstrate the feasibility of preparing transportable co-polarized frozen substrate mixtures after annihilation of the non-persistent radicals in the solid state.

CONCLUSION

We conclude that co-polarization of a substrate mixture containing $[1-^{13}\text{C}]$ butyric acid and $[1-^{13}\text{C}]$ pyruvic acid following UV-irradiation is possible and leads to a sufficiently high polarization to measure *in vivo* myocardial metabolism. It enables noninvasive and simultaneous monitoring of separate metabolic pathways in a single experiment, without addition of persistent radicals or glassing solvents.

Supplementary Material

Refer to Web version on PubMed Central for supplementary material.

Acknowledgments

This work is supported by the Swiss National Science Foundation (grant PP00P2_133562, 31003AB_131087, 310030_138146, 310030_163050 / 1, and PZ00P3_167871), the Emma Muschamp Foundation, the CIBM of the UNIL, UNIGE, HUG, CHUV, EPFL, and the Leenaards and Jeantet Foundations. Dr. Merritt was supported by R21 EB016197 and R01 DK105346. This work is part of a project that has received funding from the European Research Council (grant agreement No 682574).

References

1. Ardenkjaer-Larsen JH, Fridlund B, Gram A, Hansson G, Hansson L, Lerche MH, Servin R, Thaning M, Golman K. Increase in signal-to-noise ratio of $> 10,000$ times in liquid-state NMR. *Proc Natl Acad Sci U S A*. 2003; 100(18):10158–10163. [PubMed: 12930897]
2. Golman K, in't Zandt R, Thaning M. Real-time metabolic imaging. *Proceedings of the National Academy of Sciences of the United States of America*. 2006; 103(30):11270–11275. [PubMed: 16837573]
3. Brindle KM. Imaging Metabolism with Hyperpolarized C-13-Labeled Cell Substrates. *Journal of the American Chemical Society*. 2015; 137(20):6418–6427. [PubMed: 25950268]
4. Comment A. Dissolution DNP for in vivo preclinical studies. *J Magn Reson*. 2016; 264:39–48. [PubMed: 26920829]
5. Comment A, Merritt ME. Hyperpolarized magnetic resonance as a sensitive detector of metabolic function. *Biochemistry*. 2014; 53(47):7333–7357. [PubMed: 25369537]
6. Keshari KR, Wilson DM. Chemistry and biochemistry of ^{13}C hyperpolarized magnetic resonance using dynamic nuclear polarization. *Chem Soc Rev*. 2014; 43(5):1627–1659. [PubMed: 24363044]

7. Yoshihara HA, Bastiaansen JA, Berthonneche C, Comment A, Schwitter J. An Intact Small Animal Model of Myocardial Ischemia-Reperfusion: Characterization of Metabolic Changes by Hyperpolarized ^{13}C MR Spectroscopy. *Am J Physiol Heart Circ Physiol*. 2015; doi: 10.1152/ajpheart.00376.2015:ajpheart0037602015
8. Nishihara T, Yoshihara HA, Nonaka H, Takakusagi Y, Hyodo F, Ichikawa K, Can E, Bastiaansen JA, Takado Y, Comment A, Sando S. Direct Monitoring of gamma-Glutamyl Transpeptidase Activity In Vivo Using a Hyperpolarized (^{13}C) C-Labeled Molecular Probe. *Angew Chem Int Ed Engl*. 2016; 55(36):10626–10629. [PubMed: 27483206]
9. Cunningham CH, Lau JY, Chen AP, Geraghty BJ, Perks WJ, Roifman I, Wright GA, Connelly KA. Hyperpolarized ^{13}C Metabolic MRI of the Human Heart: Initial Experience. *Circ Res*. 2016; 119(11):1177–1182. [PubMed: 27635086]
10. Nelson SJ, Kurhanewicz J, Vigneron DB, Larson PE, Harzstark AL, Ferrone M, van Criekinge M, Chang JW, Bok R, Park I, Reed G, Carvajal L, Small EJ, Munster P, Weinberg VK, Ardenkjaer-Larsen JH, Chen AP, Hurd RE, Odegardstuen LI, Robb FJ, Tropp J, Murray JA. Metabolic Imaging of Patients with Prostate Cancer Using Hyperpolarized [^{13}C]Pyruvate. *Sci Transl Med*. 2013; 5(198):198ra108.
11. Kurhanewicz J, Vigneron DB, Brindle K, Chekmenev EY, Comment A, Cunningham CH, Deberardinis RJ, Green GG, Leach MO, Rajan SS, Rizi RR, Ross BD, Warren WS, Malloy CR. Analysis of cancer metabolism by imaging hyperpolarized nuclei: prospects for translation to clinical research. *Neoplasia*. 2011; 13(2):81–97. [PubMed: 21403835]
12. Malloy CR, Merritt ME, Sherry AD. Could ^{13}C MRI assist clinical decision-making for patients with heart disease? *NMR Biomed*. 2011; 24(8):973–979. [PubMed: 21608058]
13. Neubauer S. The failing heart--an engine out of fuel. *New England Journal of Medicine*. 2007; 356:1140–1151. [PubMed: 17360992]
14. Bastiaansen JA, Merritt ME, Comment A. Measuring changes in substrate utilization in the myocardium in response to fasting using hyperpolarized [^{13}C]butyrate and [^{13}C]pyruvate. *Sci Rep*. 2016; 6:25573. [PubMed: 27150735]
15. Ardenkjaer-Larsen JH, Leach AM, Clarke N, Urbahn J, Anderson D, Skloss TW. Dynamic Nuclear Polarization Polarizer for Sterile Use Intent. *NMR Biomed*. 2011; 24(8):927–932. [PubMed: 21416540]
16. Eichhorn TR, Takado Y, Salameh N, Capozzi A, Cheng T, Hyacinthe JN, Mishkovsky M, Roussel C, Comment A. Hyperpolarization without persistent radicals for in vivo real-time metabolic imaging. *Proc Natl Acad Sci U S A*. 2013; 110(45):18064–18069. [PubMed: 24145405]
17. Capozzi A, Hyacinthe JN, Cheng T, Eichhorn TR, Boero G, Roussel C, van der Klink JJ, Comment A. Photoinduced Nonpersistent Radicals as Polarizing Agents for X-Nuclei Dissolution Dynamic Nuclear Polarization. *Journal of Physical Chemistry C*. 2015; 119(39):22632–22639.
18. Capozzi A, Cheng T, Boero G, Roussel C, Comment A. Thermal annihilation of photo-induced radicals following dynamic nuclear polarization to produce transportable frozen hyperpolarized ^{13}C -substrates. *Nat Commun*. 2017; 8:15757. [PubMed: 28569840]
19. Cheng T, Capozzi A, Takado Y, Balzan R, Comment A. Over 35% liquid-state ^{13}C polarization obtained via dissolution dynamic nuclear polarization at 7 T and 1 K using ubiquitous nitroxyl radicals. *Physical Chemistry Chemical Physics*. 2013; 15(48):20819–20822. [PubMed: 24217111]
20. Comment A, van den Brandt B, Uffmann K, Kurdzesau F, Jannin S, Konter JA, Hautle P, Wenckeback WT, Gruetter R, van der Klink JJ. Design and performance of a DNP prepolarizer coupled to a rodent MRI scanner. *Concepts in Magnetic Resonance Part B: Magnetic Resonance Engineering*. 2007; 31B(4):255–269.
21. Yoshihara HA, Can E, Karlsson M, Lerche MH, Schwitter J, Comment A. High-field dissolution dynamic nuclear polarization of [^{13}C]pyruvic acid. *Phys Chem Chem Phys*. 2016; 18(18):12409–12413. [PubMed: 27093499]
22. Cheng T, Mishkovsky M, Bastiaansen JAM, Ouari O, Hautle P, Tordo P, van den Brandt B, Comment A. Automated transfer and injection of hyperpolarized molecules with polarization measurement prior to in vivo NMR. *NMR Biomed*. 2013; 26(11):1582–1588. [PubMed: 23893539]

23. Comment A, van den Brandt B, Uffmann K, Kurdzesau F, Jannin S, Konter JA, Hautle P, Wenckebach WT, Gruetter R, van der Klink JJ. Design and performance of a DNP prepolarizer coupled to a rodent MRI scanner. *Concepts In Magnetic Resonance Part B-Magnetic Resonance Engineering*. 2007; 31B(4):255–269.
24. Cheng T, Capozzi A, Takado Y, Balzan R, Comment A. Over 35% liquid-state ¹³C polarization obtained via dissolution dynamic nuclear polarization at 7 T and 1 K using ubiquitous nitroxyl radicals. *Phys Chem Chem Phys*. 2013; 15(48):20819–20822. [PubMed: 24217111]
25. Bastiaansen JA, Cheng T, Lei H, Gruetter R, Comment A. Direct noninvasive estimation of myocardial tricarboxylic acid cycle flux in vivo using hyperpolarized C magnetic resonance. *Journal of Molecular and Cellular Cardiology*. 2015; 87:129–137. [PubMed: 26297113]
26. Bastiaansen JAM, Cheng T, Mishkovsky M, Duarte JMN, Comment A, Gruetter R. In vivo enzymatic activity of acetylCoA synthetase in skeletal muscle revealed by ¹³C turnover from hyperpolarized [1-¹³C]acetate to [1-¹³C]acetylcarnitine. *Biochimica Et Biophysica Acta*. 2013; 1830(8):4171–4178. [PubMed: 23545238]
27. Gruetter R, Tkac I. Field mapping without reference scan using asymmetric echo-planar techniques. *Magnetic Resonance in Medicine*. 2000; 43(2):319–323. [PubMed: 10680699]
28. Staewen RS, Johnson AJ, Ross BD, Parrish T, Merkle H, Garwood M. 3-D Flash Imaging Using a Single Surface Coil and a New Adiabatic Pulse, Bir-4. *Investigative Radiology*. 1990; 25(5):559–567. [PubMed: 2345088]
29. Shaka AJ, Keeler J, Frenkiel T, Freeman R. An Improved Sequence for Broad-Band Decoupling - Waltz-16. *Journal of Magnetic Resonance*. 1983; 52(2):335–338.
30. Bastiaansen JAM, Yoshihara HAI, Takado Y, Gruetter R, Comment A. Hyperpolarized ¹³C lactate as a substrate for in vivo metabolic studies in skeletal muscle. *Metabolomics*. 2014; 10(5):986–994.
31. Comment A. The benefits of not using exogenous substances to prepare substrates for hyperpolarized MRI. *Imaging in Medicine*. 2014; 6(1):1–3.
32. Ball DR, Rowlands B, Dodd MS, Le Page L, Ball V, Carr CA, Clarke K, Tyler DJ. Hyperpolarized butyrate: a metabolic probe of short chain fatty acid metabolism in the heart. *Magn Reson Med*. 2014; 71(5):1663–1669. [PubMed: 23798473]
33. Knowles SE, Jarrett IG, Filsell OH, Ballard FJ. Production and utilization of acetate in mammals. *Biochem J*. 1974; 142(2):401–411. [PubMed: 4441381]
34. Bornet A, Milani J, Vuichoud B, Linde AJP, Bodenhausen G, Jannin S. Microwave frequency modulation to enhance Dissolution Dynamic Nuclear Polarization. *Chemical Physics Letters*. 2014; 602:63–67.

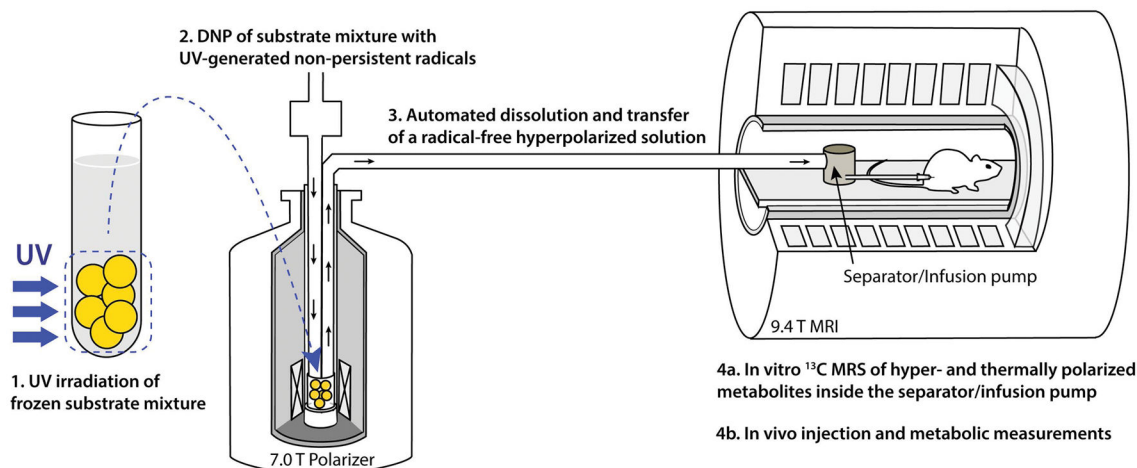


Figure 1.

Illustration of the *in vivo* and *in vitro* experimental method based on UV-irradiated ^{13}C -labeled metabolic substrate mixtures: (1) a frozen mixture of ^{13}C -labeled substrates, in this case $[1-^{13}\text{C}]$ butyric and $[1-^{13}\text{C}]$ pyruvic acids, is irradiated with UV light at 77 K; (2) the mixture is loaded into a DNP polarizer and ^{13}C nuclei are dynamically polarized for 1–2 h; (3) using an automated process, the sample is quickly dissolved in superheated buffer solution and automatically transferred from the polarizer into a separator/injection pump located inside the bore of an MRI magnet; (4a & 4b) *in vitro* ^{13}C MRS measurements are performed while the hyperpolarized ^{13}C -substrate mixture is inside the separator/injection pump and/or the mixture is injected into the rat via a femoral vein catheter and *in vivo* hyperpolarized ^{13}C MRS measurements are launched.

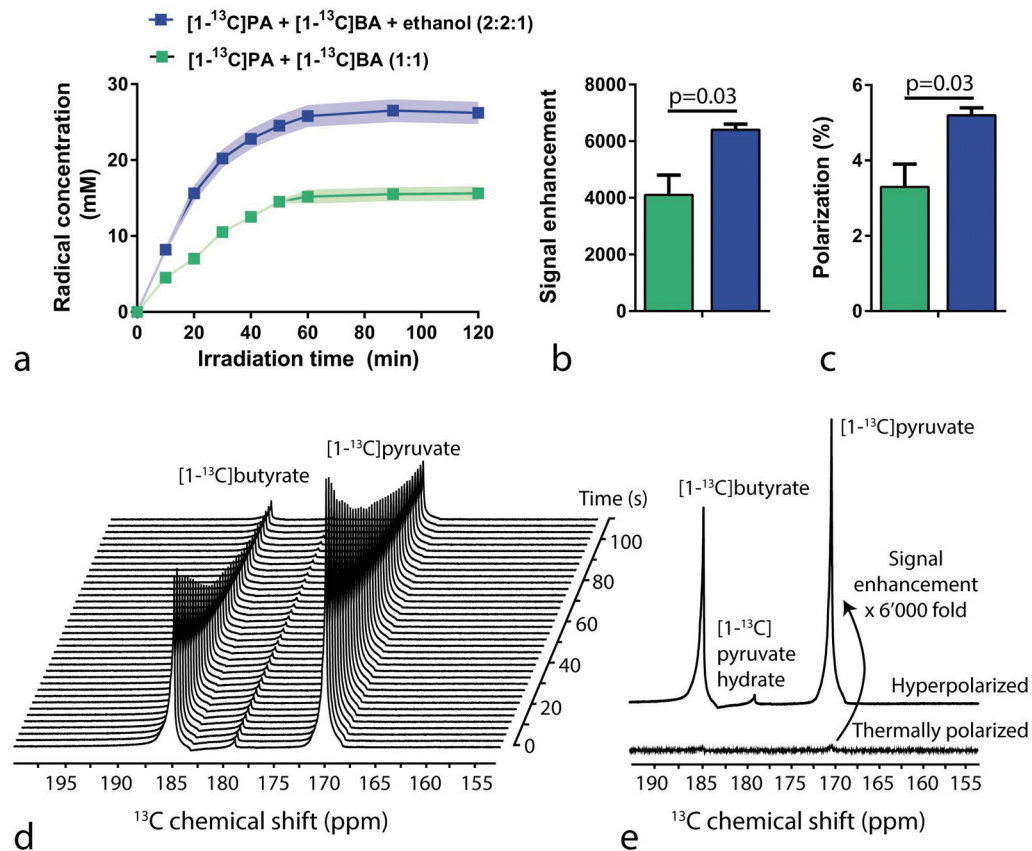
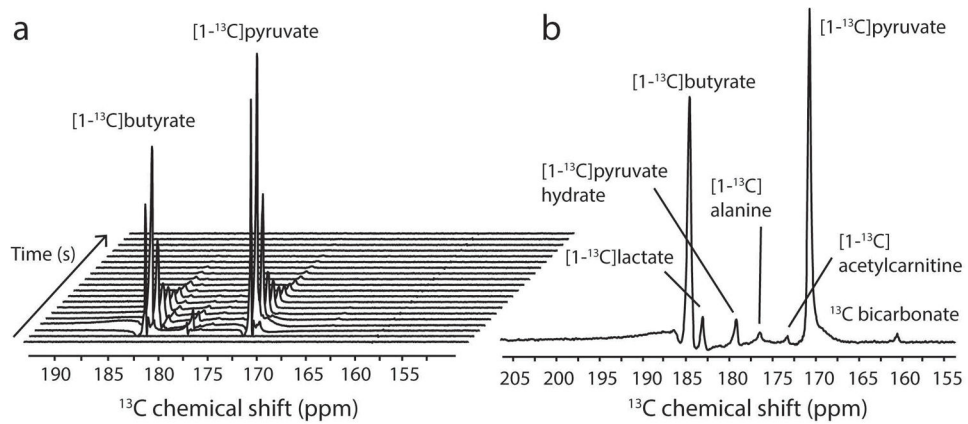


Figure 2.

a) Radical concentration as a function of the UV light irradiation time for two different mixtures: $[1-^{13}\text{C}]\text{pyruvic-}$ and $[1-^{13}\text{C}]\text{butyric}$ acids in a 1:1 volume ratio (green), and the same with the addition of ethanol (blue). Signal intensity enhancement (b) and polarization levels (c) of pyruvic acid using two differently prepared mixtures. (d,e) *In vitro* hyperpolarized ^{13}C MRS of the UV-irradiated mixture of ^{13}C labeled substrates. (d) A hyperpolarized ^{13}C spectral time course of the mixture measured in the infusion pump inside the MRI scanner after dissolution and automated sample transfer. Hyperpolarized spectra were acquired with an RF excitation angle of 5° and repetition time TR of 3 s. (e) The first measured hyperpolarized ^{13}C spectrum after dissolution (top spectrum) was compared to its thermally polarized counterpart (bottom spectrum) to calculate the SNR enhancement in liquid state. A 6'000 fold signal enhancement was measured. All spectra are displayed without spectral line broadening.

**Figure 3.**

In vivo ^{13}C MRS measured in the healthy myocardium after the injection of a hyperpolarized UV-irradiated $[1-^{13}\text{C}]$ pyruvate/ $[1-^{13}\text{C}]$ butyrate mixture. (A) Representative ^{13}C spectral time course following the injection of the substrate mixture. Acquisitions were respiratory-gated and cardiac-triggered with a repetition time of 3 s and a flip angle of 30° . (B) Sum of the 15 spectra acquired starting 9 s after dissolution. The myocardial metabolism of both pyruvate and butyrate could be observed through the formation of alanine, lactate, bicarbonate and acetylcarnitine.

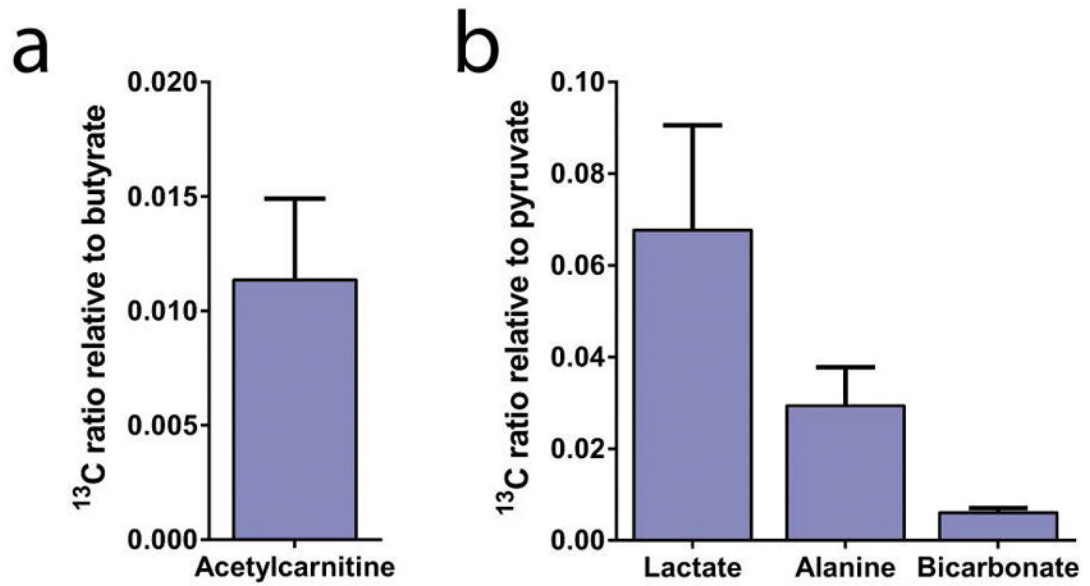


Figure 4. ^{13}C metabolite signal integral ratios relative to their respective injected substrate following the injection and myocardial metabolism of a UV-irradiated radical-free mixture of $[1-^{13}\text{C}]$ pyruvic acid and $[1-^{13}\text{C}]$ butyric acid.

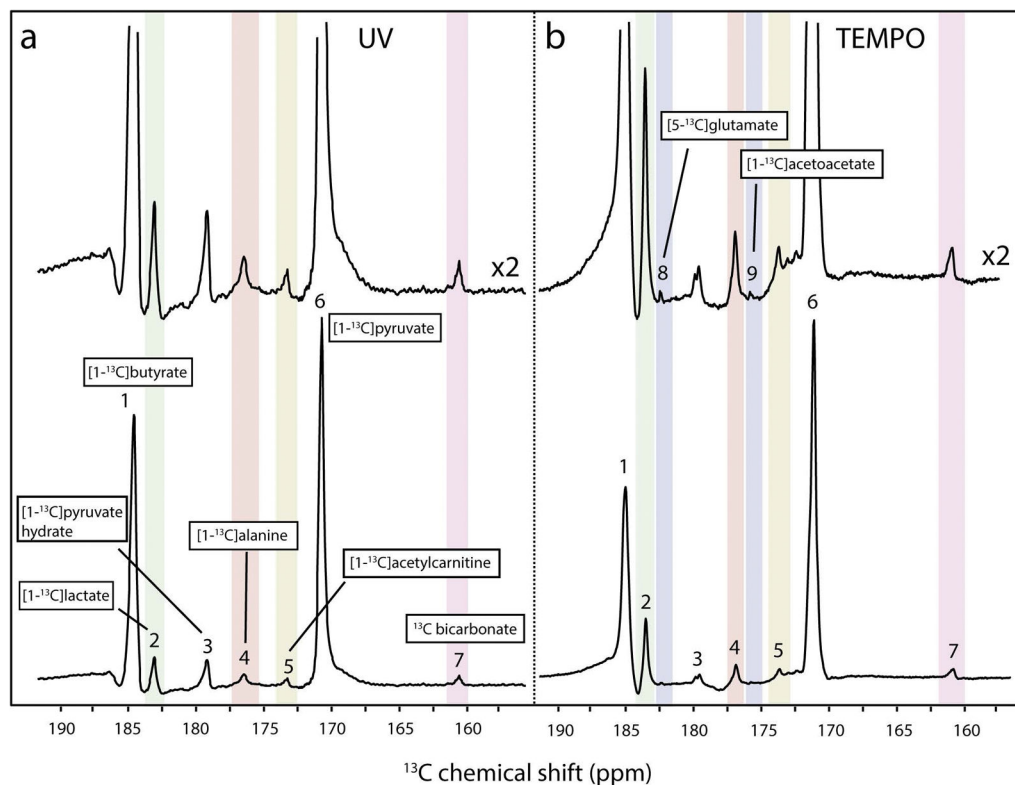


Figure 5.

Comparison of spectra acquired *in vivo* after the administration of a UV-irradiated mixture containing [1- ^{13}C]pyruvate and [1- ^{13}C]butyrate (left panel) and the administration of a mixture of [1- ^{13}C]pyruvate and [1- ^{13}C]butyrate containing TEMPO persistent radicals (right panel). Data obtained using TEMPO radicals was presented in an earlier publication (14). Spectra in the top panels were scaled with factor 2. Observed metabolites are indicated as follows: 1, [1- ^{13}C]butyrate; 2, [1- ^{13}C]lactate; 3, [1- ^{13}C]pyruvate hydrate; 4, [1- ^{13}C]alanine; 5, [1- ^{13}C]acetylcarnitine; 6, [1- ^{13}C]pyruvate; 7, ^{13}C -bicarbonate; 8, [5- ^{13}C]glutamate; 9, [1- ^{13}C]acetoacetate.